 doi:10.20944/preprints201707.0078.v1

Title

An *In Silico* Study of a Novel rpoB Insertion in a Cluster of Clinical Strains of *Mycobacterium tuberculosis* Highly-Rifampicin Resistant

Author names and affiliations

Maria Lucia R. Rossetti[1,2#], Pedro Almeida da Silva[3#], Raquel Maschmann[4], Andrea von Groll [3], Leonardo S. Esteves[2], Fernanda S. Spies[4], Evelin Sabini[2], Rubia Raubach Trespach[5], Elis R. Dalla Costa[1], Hermes Luís Neubauer de Amorim[2,5]

[1]Fundação Estadual de Produção e Pesquisa em Saúde - FEPPS - Porto Alegre, RS, Brazil.

[2]Programa de Pós-Graduação em Biologia Celular e Molecular Aplicada a Saúde, Universidade Luterana do Brasil (ULBRA/RS), Canoas, RS, Brazil.

[3]Núcleo de Pesquisa em Microbiologia Médica (NUPEMM), Faculdade de Medicina, Universidade Federal do Rio Grande, Rio Grande, RS, Brazil

[4]Programa de Pós-Graduação em Biologia Celular e Molecular, Centro de Biotecnologia, Universidade Federal do Rio Grande do Sul (UFRGS), Porto Alegre, RS, Brazil

[5]Laboratório de Bioinformática Estrutural, Universidade Luterana do Brasil (ULBRA/RS), Canoas, RS, Brazil.

[#]Contributed equally.

Corresponding author

Hermes Luis Neubauer de Amorim

Tel.: +555134774000 ext 2774
Fax: +555134779239
e-mail: hermes.amorim@ulbra.br

 doi:10.20944/preprints201707.0078.v1

ABSTRACT

Rifampicin is one of the most important chemotherapeutic agents used in the treatment of tuberculosis. *M. tuberculosis* clinical strains resistant to rifampicin harbor mainly mutation in an 81-base pair region of *rpoB*. These mutations mainly consist of single amino acid substitutions. However insertions also can be related with rifampicin resistance strains. Herein, we described an insertion of 12 nucleotides in clinical isolates of *M. tuberculosis* resistant to rifampicin, all obtained from inmates. To evaluate the importance this insertion in surviving and drug resistance, it were carried out fitness experimental assays as well as *in silico* studies of 3D structural models, molecular docking simulations and virtual screening. The medical records of the seven patients showed all were previously treated to tuberculosis. Growth curves shown that the insertion determines a biological cost when compared to wild type *rpoB* and *katG*; or the double mutated *rpoB* S531L and *katG* S315T. From docking and molecular dynamics simulations it can be inferred that the insertion does not affect the process of synthesis of RNA transcripts. On the other hand, in the mutant RNAP-RIF complex rifampicin confirmed a low affinity interaction for the mutant form. Interesting, virtual screening for potential inhibitors for wtRNAP and mRNAP using a library of 1446 compounds approved by the FDA showed that the best ligands were mainly compounds with antibiotic activity, although the targets involved in the pharmacological action are other than RNAP. In conclusion, seven strains of *M. tuberculosis* RIF resistant that present an insertion of four amino acids in RNA polymerase showed by growth curve assays, a biological cost. Further, bioinformatics tools had characterized the putative drug resistance dynamic as well as the maintenance of RNA polymerase activity.

 doi:10.20944/preprints201707.0078.v1

KEYWORDS

Rifampicin; insertion; biological cost; *M. tuberculosis*; resistance; structural bioinformatics

 doi:10.20944/preprints201707.0078.v1

1. INTRODUCTION

Tuberculosis (TB) is an infectious disease caused by *Mycobacterium tuberculosis*. According to World Health Organization, Brazil is among the High Burden Countries, the 22 countries responsible for more than 80% of the TB in the world (WHO, 2016). The number of TB patients diagnosed and treated for MDR-TB (TB with strains resistant to rifampicin-RIF and isoniazid-INH) is increasing worldwide and treatment success rates in patients with drug-resistant TB remain unacceptably low (World Health Organization, 2010).

Although treatment of both, MDR and XDR-TB (MDR-TB also resistant to any fluoroquinolone and at least one of three injectable second-line drugs) strains resistant is possible with available drugs the treatment course is substantially more costly, toxic and longer than drug-susceptible TB, with higher rates of treatment failure and mortality (Gandhi et al., 2010). In fact, the current efforts to control of TB have been threatened by the increase of TB cases with drug resistance strains (BIADGLEGNE et al., 2015; Daley and Horsburgh, 2014; Diel et al., 2014; Frieden et al., 2014; Murray et al., 2014; Sotgiu et al., 2015; Strehl, 2014).

Resistance to antituberculosis drugs arises mainly as a result of spontaneous mutations in the genome of *M. tuberculosis*, these resistance-conferring mutations occur mainly at predictable rates for each antituberculosis drug (e.g. INH 10^{-6} and RIF 10^{-8}) (Almeida Da Silva and Palomino, 2011; Zhang and Yew, 2009). Thus, in patients with active TB disease, subpopulations of resistant mycobacteria spontaneously arise and in the presence of drug-selection pressure, drug-resistant organisms multiply and could become the dominant strain (Gandhi et al., 2010).

 doi:10.20944/preprints201707.0078.v1

The acquisition of drug resistance in bacteria can determine a biological cost in terms of reduced growth rate, virulence and transmissibility. However, several studies have showed that in general clinical resistant strains grow and are transmitted as well as the susceptible strains (Borrell and Gagneux, 2009; de Vos et al., 2013; Spies et al., 2013).

RIF is one of the most important chemotherapeutic agents used in the TB treatment; RIF binds to the beta-subunit of the RNA polymerase encoded by the *rpoB* gene and inhibits transcription (Cole, 1996). More than 95% of *M. tuberculosis* clinical strains resistant to RIF harbor mutation in an 81-base pair region of *rpoB* known as the RIF resistance determining region (RRDR) (Almeida Da Silva and Palomino, 2011). These mutations mainly consist of single amino acid substitutions (Gill and Garcia, 2011; Herrera et al., 2003). However, other molecular alterations can be related with RIF resistance, as the insertion observed in *M. smegmatis* (Malshetty et al., 2010).

As part in our studies with patients that do not comply with the TB treatment, we have sequenced a large number of the *rpoB* and *katG* genes to correlate with the treatment failure (data not published yet). During the course of this study we have found the most frequent mutations related with RIF-resistance, however we found in seven strains RIF resistant an insertion of 12 nucleotides (4 amino acids) isolated from inmates. This insertion, result of the duplication of codons 517-520 (QNNP amino acid sequence) in the *rpoB* gene of the bacillus, is implicated as being responsible for the RIF resistance. Further, these strains seem to be transmitted in this community, as all seven patients have the same MIRU-VNTR 24-loci pattern.

The understanding of the molecular mechanism involved in RIF resistance may contribute to the discovery and design of new molecules for the treatment of rifampicin-resistant TB. However, until now the crystal structure of RNA polymerase from *M.*

 doi:10.20944/preprints201707.0078.v1

tuberculosis has not been determined. This kind of structural information is important to better understand the molecular mechanisms of resistance-causing mutations and allow efforts in structure-drug based design. Thus, in order to address this issue and as the first stage of the *in silico* investigation, 3D structural models of the wild-type (wt) and mutant RNA polymerases (RNAPs) from *M. tuberculosis* were built using a combination of the techniques of homology modeling and molecular dynamics simulations.

Homology modeling is a computational technique used to build three dimensional (3D) structures of protein targets from structural templates which are, in turn, experimental structures of homologous proteins (Liu et al., 2011). The validity of the technique is based on the principle that similarity between primary structures of proteins (amino acid sequences) imply similarity in 3D structures (Aloy et al., 2003; Chothia and Lesk, 1986).

Molecular dynamics (MD) simulation is a technique used to calculate the time-dependent behavior of a molecular system. The central idea underlying the MD simulation method is that the behavior of a system can be investigated by monitoring the detailed behavior of all particles that constitute the system (Rapaport, 2013). MD simulation can be used, as intended in this study, to generate more realistic models for proteins in solution (Kerrigan, 2013; van Gunsteren et al., 2008).

After obtaining the RNAP structural models, the complexes between wt and mutant RNAPs with rifampicin were generated by molecular docking simulations. The latter is a technique used to address the question of whether and how one molecule will bind to another molecule, allowing investigation of, for example, drug-receptor interactions (Ferreira et al., 2015; Guedes et al., 2014). Finally, as a preliminary study, a

 doi:10.20944/preprints201707.0078.v1

virtual screening (VS) study was conducted to identify potential inhibitors of the mutant form of RNA polymerase.

The methodology described here is very similar, except regarding to VS, to that successfully used in previous work conducted by our group on the generation of structural models of wild type and mutant forms of arylamine-N-acetyltransferase of *M. tuberculosis* (Coelho et al., 2011; Ramos et al., 2012).

2. MATERIAL AND METHODS

2.1 Strains and culture conditions

The strains that presented the insertion in the *rpoB* obtained from inmates of State Penitentiary of Jacuí (PEJ), city of Charqueadas, South of Brazil were selected for this study and the medical records were analyzed. After the primary isolation and characterization the strains were cultured in Ogawa-Kudoh media and frozen in 7H9 plus glycerol 10% for further experiments.

2.2 MIC determination

The resazurin microtiter assay (REMA) was used for MIC determination (Palomino et al., 2002) of RIF (16 µg/ml to 0.03 µg/ml), and INH (12.8 µg/ml to 0.01 µg/ml). The breakpoint used to determine RIF and INH resistance was an MIC of > 0.25 µg/ml (Cui et al., 2013).

2.3 DNA Extraction and sequencing

DNA isolation and amplification of genes regions were carried out as described previously (Dalla Costa et al., 2009; Telenti et al., 1993; van Soolingen et al., 1994). Sequencing was performed in the ABI Prism 3100 DNA sequencer (Applied

 doi:10.20944/preprints201707.0078.v1

Biosystems). Nucleotide sequences were analyzed using the programs PREGAP and GAP4 of the STADEN software package ver. 10.0. Nucleotide sequences with Phred values >20 were considered for analysis.

2.4 Genotyping

Spoligotyping was performed using a commercial kit (Isogen Biosciences B.V., The Netherlands) according to the manufacturer's instructions. The Shared International Types (SITs) and families were identified according to the SpolDB4 (Brudey et al., 2006). The strains were further characterized by the MIRU-VNTR 24 loci (Supply et al., 2006).

2.5 Determination of growth curve by resazurin reduction method

The growth curve was determined by resazurin reduction method as previously reported (von Groll et al., 2010b). Briefly, the two individual clinical isolates with the insertion, three wild type clinical isolates and in one susceptible control strain (H37Rv) were freshly sub-cultured on Löwenstein-Jensen medium and kept for 3 weeks. An inoculum was prepared at a turbidity of a McFarland tube No.0.5 in ultra pure water and further diluted 1:10 in Middlebrook 7H9 broth supplemented with 0.1% casitone, 0.5% glycerol, and 10% OADC (oleic acid, albumin, dextrose and catalase) (Becton-Dickinson, USA). Resazurin sodium salt powder (Acros Organic NV, Belgium) was prepared at 0.02% (wt/vol) in distilled water, sterilized by filtration and stored at 4 °C. The REMA method was performed in a sterile flat-bottom 96-well plate in which was added: 200 µL of sterile distilled water in all peripheral wells, 200 µL of 7H9 medium containing 10% OADC in three wells (negative control) and 100 µL of 7H9 with OADC + 100 µL of the inoculum of each strain in another three wells. The plate was

 doi:10.20944/preprints201707.0078.v1

closed with its lid, put in sealed plastic bags and incubated at 37°C. After 48 hours, 30 µL of 0.02% resazurin was added to the wells. The plate was re-incubated at 37 °C and every 24 hours the OD of each well was measured using a plate reader (Biotrak II Visible Plate) at a wavelength of 620 nm. Resazurin is blue and the OD decreases according to the change in colour to pink due to the bacterial metabolism. In order to establish the growth curves, the difference in OD between the average of three wells of the inoculated and the control (uninoculated wells) was plotted versus the time of incubation. The fitness of each strain was estimated by the growth index (GI) which was the time needed by each strain to reach an OD of 0.4 starting at an OD of 0.2. This time was calculated from the growth curve considering that all strains were in the logarithmic phase of growth between the two OD values.

The biological cost was determined by the fitness relative (FR) which is the ratio of the GI of the insertion *rpoB* isolates in relation to the H37Rv and in relation to the wild-type. A biological cost was considered if the FR was > 1.

2.6 Homology modeling

Protein structure models were generated using MODELLER program (Eswar et al., 2008). Typically, 100 models were generated for each RNAP (wild type and mutant). The model with the lowest energy DOPE (discrete optimized potential energy) (Shen and Sali, 2006) score was selected for the subsequent steps. The structural model generated for the wild type RNA polymerase of *M. tuberculosis* was restricted to the subunits β (RpoB) and β´ (RpoC).

The amino acid sequences deposited in the NCBI under accession numbers NP_215181.1 and NP_215182.1 corresponding, respectively, to the subunits β and β' were selected for this procedure. Each subunit was modeled separately. The subunit β

 doi:10.20944/preprints201707.0078.v1

was generated using three structures as templates, corresponding to the β subunits in the crystallographic structures of RNA polymerases from *Thermus thermophilus* (deposited as code 1IW7 (Vassylyev et al., 2002) in the Protein Data Bank, PDB (Berman, 2000; Rose et al., 2017) and *Thermus aquaticus* (deposited as PDB codes 1HQM (Minakhin et al., 2001) and 1YNJ). Three templates were used in order to reduce the number of gaps in the alignment between the target and the template sequences. The subunit β' was generated using a single template, the β' subunit of RNA polymerase from *T. thermophilus* (PDB accession code 1IW7). Subsequently, the β and β' subunits were joined by fitting these with the respective subunits of the experimental structure of the RNAP from *T. aquaticus*. The final model of wtRNAP was then refined until stabilization by molecular dynamics simulation.

The structural model of the mutant form of RNA polymerase was generated using as template the refined model of wtRNAP. The stereochemical quality of the wtRNAP and mRNAP models was evaluated during the modeling process using PROCHECK (Laskowski et al., 1993) (Lüthy et al., 1992)VERIFY3D and (Colovos and Yeates, 1993)ERRAT, implemented in SAVES ("SAVES - The Structure Analysis and Verification Server," n.d.)

2.7 Molecular Dynamics Simulations

Molecular dynamics simulations were carried out using GROMOS96 53a6 force field(Oostenbrink et al., 2004) implemented in GROMACS package (Pronk et al., 2013), version 4.5.4. Parameters used in the simulations of the complexes were the same described for the uncomplexed RNAPs. In order to obtain more reliable information on rifampicin-protein interactions the simulations of the complexes were carried out in triplicate, each replicate different only in their initially assigned

 doi:10.20944/preprints201707.0078.v1

velocity distributions. Taking into consideration that the pKa value of the N3 piperazine nitrogen of rifampicin is 7.9, the protonated form of this group was used in docking calculations (section 2.8) and in the molecular dynamics simulations of the complexes. All systems were simulated in NPT ensemble and periodic boundary conditions. The dimensions of the central box were chosen in such way that the minimum distance of any protein atom to the closest box wall was 12 Å. The simulations were carried out using explicit solvent water molecules described by the simple point charge (SPC) model (Berendsen et al., 1987). Initially, the protein or complex structure in each system was submitted to a maximum of 500 steps of steepest descent energy minimization. To relax strong solvent-solvent and solvent-protein non-bonded interactions, 100 ps of MD simulation was performed restraining the protein structure. Counter ions were added to neutralize the systems. Initial velocities were assigned according to Maxwell distribution. After the equilibrium stage the MD simulations were run using an integration time step of 2 ps. Each system was heated with gradual increments in the following temperatures: 150 K (1ns), 200 K (1ns), and 250 K (1ns). After, the temperatures of the systems were adjusted to 309.15 K. The temperatures of solvent and solutes (protein, ligands, and heme group) were independently coupled to a thermal bath with a relaxation time of 0.1 ps using the v-rescale thermostat (Bussi et al., 2007). The pressure in the systems was weakly coupled to a pressure bath of 1 atm applying an isotropic scaling and 0.5 ps of relaxation time using the Parrinello-Rahman barostat (Parrinello and Rahman, 1981). Bond lengths were constrained using the LINCS algorithm (Hess et al., 1997) with 4th order expansion. Electrostatic interactions among non-ligand atoms were evaluated by the smooth particle mesh Ewald (SPME) (Essmann et al., 1995) with a charge grid spacing of approximately 1.2 Å.

 doi:10.20944/preprints201707.0078.v1

The charge grid was interpolated on a cubic grid with the direct sum tolerance set to 4.0×10^{-6}. Lennard-Jones interactions were evaluated using a 10 Å atom-based cutoff. The pair list was updated at each 10 steps.

2.8 Docking

All docking procedures utilized the Autodock 4.2 package (Morris et al., 2009, 1998) Protein and ligand were prepared for docking simulations with AutoDock Tools (ADT), version 1.5.4 (Sanner, 1999). All water molecules were removed from the original RNAP files. Protein was considered rigid whereas the ligand was considered flexible. Gasteiger (Gasteiger and Marsili, 1980) partial charges were calculated after addition of all hydrogens. Nonpolar hydrogens of protein and ligand were subsequently merged. A grid box of 60 × 60 × 60 points with a spacing of 0.35 Å was centered on the C_δ of the Gln403 of the subunit β. The global search Lamarckian genetic algorithm (LGA) (Morris et al., 1998) and the local search (LS) pseudo-Solis and Wets (Solis and Wets, 1981) methods were applied in the docking search. The standard docking protocol for rigid and flexible ligand docking consisted of 100 independent runs, using an initial population of 50 randomly placed individuals, with 2.5×10^6 energy evaluations, a maximum number of 27000 iterations, a mutation rate of 0.02, a crossover rate of 0.80, and an elitism value of 1. The probability of performing a local search on an individual in the population was 0.06, using a maximum of 300 iterations per local search. The resulting docked conformations were clustered into families according to the RMSD. The lowest docking-energy conformation of the cluster with lowest energy was chosen as initial structure for the molecular dynamics simulations of the RNAP-rifampicin complexes.

 doi:10.20944/preprints201707.0078.v1

All molecular figures were generated using Chimera software (Pettersen et al., 2004).

2.9 Virtual screening

The screening of potential inhibitors of mutant RNAP was performed using the AutoDock Vina (Trott and Olson, 2009) implemented in PyRx interface (Virtual Screening Tool) (Dallakyan and Olson, 2015). In the study were evaluated 1446 compounds approved by the Food and Drug Administration (FDA) obtained from the DrugBank database (Knox et al., 2011; Law et al., 2014). A grid with dimensions of 16 x 16 x 16 Å was centered on Rif-binding region of RNAP. Each ligand was subjected to five independent docking runs. The remaining parameters were the same as those used in Pyrx distribution. At the end of the docking of each ligand, the pose with lowest binding energy was stored.

3. RESULTS AND DISCUSSION

All seven strains shared the same MIRU-VNTR 24-loci profile and the same spoligotyping pattern, SIT 863, belonging to *M. tuberculosis* LAM family as previously described (Dalla Costa et al., 2015). Furthermore, all strains also have the same insertion in *rpoB* (ins 516 CCAGAACAACCC) (Figure 1) and the same mutation in the *katG* gene (S315T: AGC-ACC). Further, they showed highly-RIF resistant (MIC>16 µg/ml) and INH resistant (MIC from 3.2 to >12.8 µg/ml).

Preprints (www.preprints.org) | NOT PEER-REVIEWED | Posted: 27 July 2017 doi:10.20944/preprints201707.0078.v1

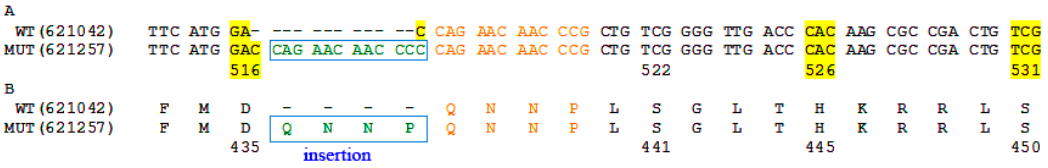

Figure 1. *RpoB* in the wild-type and in the mutated strains. A) codon sequence; B) amino acid sequence. The numbers below each sequence correspond to the wild-type sequence.

The emergence, spread and persistence of drug resistance strains reduce the successful treatment and control of TB. The evolution of single drug resistant to multiple antibiotics is driven mainly by the sequential acquisition and accumulation of resistance conferring mutations on the bacterial chromosome. Biological cost has been evaluated mainly by growth rate, being one indirect evaluation of fitness (Andersson and Hughes, 2010; von Groll et al., 2010a, 2010b).

The growth index average (GI) was determined for the two individual clinical isolates with the insertion (GI=38.5h), for three wild type clinical isolates (GI=20h) and in one susceptible control strain (H37Rv) (GI=15). The insertion isolates grow 1.95 and 2.5 slower than the wild type and H37Rv, respectively, showing a fitness disadvantage.

Molecular basis of drug-resistant *M. tuberculosis* indicates that chromosomal mutations are responsible for the majority of resistance in clinical isolates. The predominance of a mutation is the product of the probability of the mutation occurring in the genome and the probability of the altered microorganism surviving and transmitted in a given environment (Bergval et al., 2012). In this study we described a transmission of a mutated strain in seven TB patients during six years. Studding the fitness by growth curves in resazurin reduction method we observed that this mutation had a fitness cost when compared to wild type *rpoB* and *katG*; or with the double mutated *rpoB* S531L and *katG* S315T (mutations that are very frequently found in clinical isolates RIF and INH resistance).

Preprints (www.preprints.org) | NOT PEER-REVIEWED | Posted: 27 July 2017 doi:10.20944/preprints201707.0078.v1

3.1 *In silico* structural models

The sequences of the RpoB (β) and RpoC (β') subunits from *M. tuberculosis* were compared, for homology modeling purposes, with the Protein Data Bank (Berman, 2000; Rose et al., 2017) database using the BLASTp (Altschul et al., 1990) program. The most significant alignments were found to sequences from of *T. thermophilus* and *T. aquaticus*, both with 50% of identity. Based on these identities is possible to infer that the structural models generated on the basis of the crystal structures of *T. thermophilus* and *T. aquaticus* homologues are of good accuracy for bioinformatics studies (Hillisch et al., 2004). The premise for the use of these two enzymes as templates is also based on the fact that RNAPs are unambiguously closely related in structure and function independent of the organism (Ebright, 2000; Ghosh et al., 2010; Murakami and Darst, 2003). Furthermore, one crystal structure of *T. aquaticus* RNA polymerase (PDB code 1YNN) (Campbell et al., 2005) is available in complex with RIF, which aids in the interpretation and a better understanding of the results obtained in this study.

Other bacterial RNAP whose the structure in complex with RIF is available is the *E. coli* (PDB code 4KMU) (Molodtsov et al., 2013). It is interesting that in both complexes (of *T. aquaticus* and *E coli* RNA polymerases) the interaction with RIF involves the same amino acid residues. Similarly, all of the twelve residues interacting with RIF in the structure of *T. aquaticus* RNA polymerase are conserved in the *M. tuberculosis* RNA polymerase (Gln429, Leu430, Gln432, Phe433, Asp435, His445, Arg448, Ser450, Leu452, Gly453, Glu484 and Ile491) (Gill and Garcia, 2011). These findings corroborate that, as previously suggested by Campbell and co-workers

Preprints (www.preprints.org) | NOT PEER-REVIEWED | Posted: 27 July 2017 doi:10.20944/preprints201707.0078.v1

(Campbell et al., 2001), the same residues are involved in complex between RIF and RNAP from *M. tuberculosis*.

3.1 Rifampicin interaction with RNA polymerase

In order to assess potential spatial configurations for RIF in the RNAP binding site, docking simulations were performed for the wild-type and mutant forms of the polymerase (**Figure 2**). Docking of RIF on wtRNAP resulted in a binding energy of -8.19 kcal whereas on mRNAP resulted in a binding energy of -7.8 kcal.

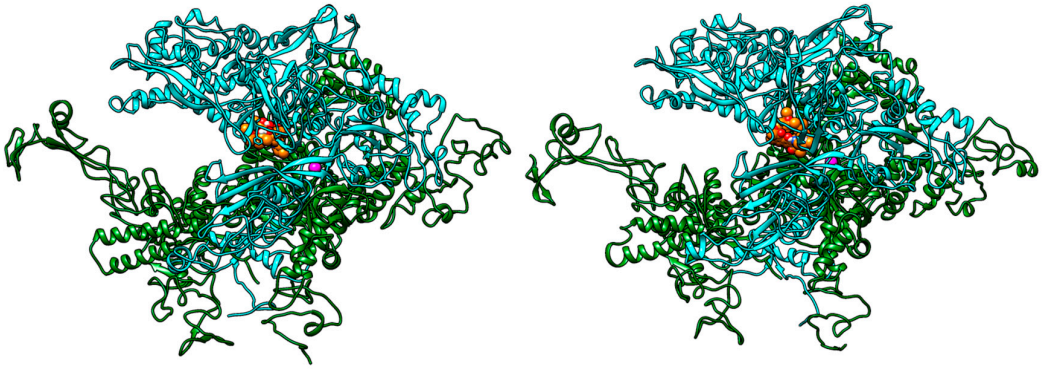

Figure 2. Schematic representations of the structural models of β and β' subunits of (A) wtRNAP and (B) mRNAP generated by homology modeling in complex with RIF. Most probable orientation of RIF in each complex determined by molecular docking. The backbone of RNAP structure is shown as ribbons (β, cyan; β', green). The Mg^{2+} ion at the active site region is shown as a magenta sphere. RIF is shown as orange spheres colored by heteroatom.

The effect of the insertion on the local structure of the Rif-binding region can be seen in **Figure 3**. It is possible to observe that the main chain of the mutant form has a local structural distortion as compared to the wtRNA, leading to a different orientation and positioning of the ligand after docking. At the same time, considering that this region is close to the active site and that the mutant polymerase remains active, it can be inferred that the **QNNP** insertion does not affect the process of synthesis of RNA transcripts.

Preprints (www.preprints.org) | NOT PEER-REVIEWED | Posted: 27 July 2017 doi:10.20944/preprints201707.0078.v1

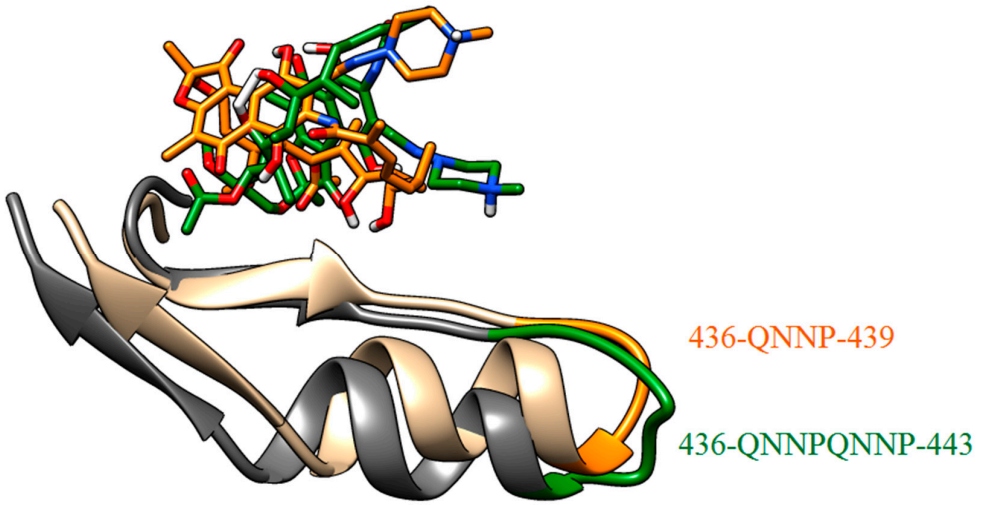

Figure 3. Schematic representation of the superposition of the RIF binding regions in wild-type and mutant forms of RNAP from *M. tuberculosis*. RIF represented as sticks and binding region represented as ribbons. wtRNAP-RIF complex: RIF colored in orange and RNAP binding region colored in beige. mRNAP-RIF complex: RIF colored in green and RNAP binding region colored in gray. Orange and green represent the insertion region in wtRNAP and mRNAP respectively. The rest of protein is not shown for clarity.

In order to verify the reproducibility of the receptor-ligand interactions predicted by docking, MD simulations of the complexes were performed in triplicate. The only variation between triplicates was the value of the random number seed used to assign the initial velocities.

In **Figure 4** it can be seen that the structure of rifampicin remained positioned in the same region in two simulations of wtRNAP-RIF complex. On the other hand, in mRNAP-RIF complex rifampicin adopted different positions in the three simulations, confirming the low affinity interaction expected for the mutant form. The observation of multiple conformations for RIF can be attributed to a disruption in the binding site due to insertion into mRNAP.

Preprints (www.preprints.org) | NOT PEER-REVIEWED | Posted: 27 July 2017 doi:10.20944/preprints201707.0078.v1

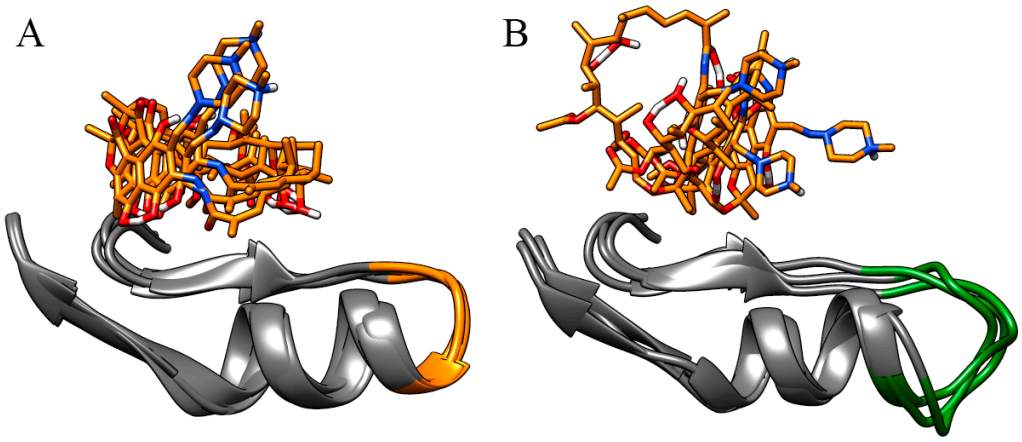

Figure 4. Superposition of the final structures (snapshots) of the MD simulations of RNAP-RIF complexes. (A) wtRNAP-RIF. (B) mRNAP-RIF. RIF is shown as orange sticks colored by heteroatom. RNAP binding region shown in ribbons: (A) region 436-QNNP-439 of wtRNAP represented in orange; (B) region 436-QNNPQNNP-443 of mRNAP represented in green. The rest of protein is not shown for clarity.

On the other hand, the final structures of the wtRNAP-RIF complexes showed contacts and the formation of hydrogen bonds with key residues of the polymerase. In **Figure 5** it is shown the model for interaction of rifampicin with wtRNAP, proposed from the analysis of the final structures of the MD simulations. Note the presence of contacts ≤ 4 Å with 13 amino acids: Arg167, Gln429, Ser431, Gln432, Phe433, Asp435, His445, Arg448, Ser450, Leu452, Pro483, Glu484 and Ile491, all of the β subunit. This *in silico* model shows RIF interacting through hydrogen bonds with four amino acids residues: Gln432 [Gln432(NεH1)-O6(RIF); Gln432(NεH2)-O11(RIF)], Phe433 [Phe433(NH)-O8(RIF)], Asp435 [Asp435(Oδ)-O10(RIF)], Ser450 [Ser450(OH)-O2(RIF)]. Three of these hydrogen bonds occur in the crystallographic complex of RNAP from *T. aquaticus* and RIF: Phe394(NH)-O8(RIF); Asp396(Oδ)-O10(RIF) and Ser411(OH)-O2(RIF). It can be observed also that the side chains of His445 and Arg448 are very close to the RIF, which may suggest the occurrence of hydrogen bonds with these residues.

Preprints (www.preprints.org) | NOT PEER-REVIEWED | Posted: 27 July 2017 doi:10.20944/preprints201707.0078.v1

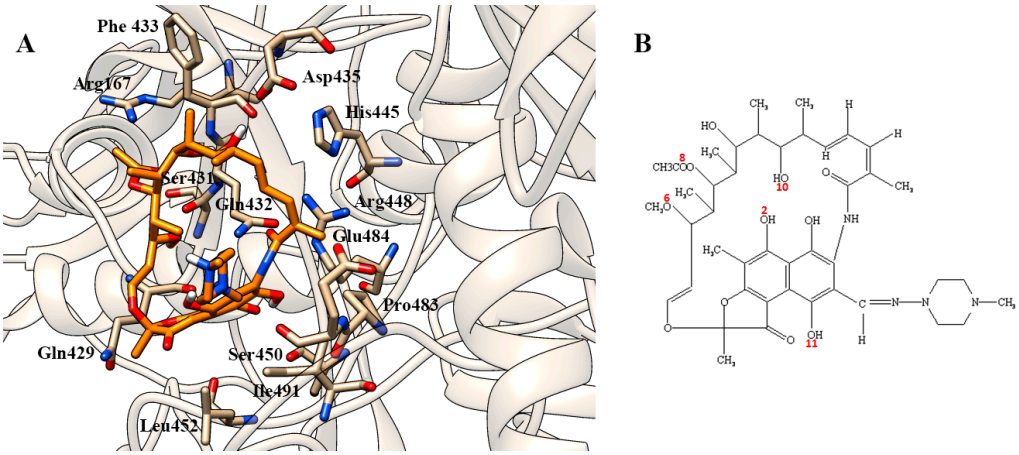

Figure 5. (A) Model of the interaction of rifampicin with the wild-type form of RNAP from *M. tuberculosis*. Rifampicin is shown as orange sticks colored by heteroatom. Amino acids represented as sticks colored by CPK. Protein represented in ribbons. (B) Structural formula of RIF.

3.2 Virtual screening

The calculations were performed with AutoDock Vina (Trott and Olson, 2009) program using a library of 1446 compounds approved by the FDA and available in the DrugBank database (Knox et al., 2011; Law et al., 2014). Virtual screening was performed on energy minimized structures of wtRNAP and mRNAP obtained from the last frame of the molecular dynamics simulations. Whereas the standard error estimate for the VS docking program used in the study is 2.75 to 2.85 kcal/mol (Trott and Olson, 2009), it can be understood that, taking as reference the binding energy of RIF, compounds with binding energy difference more favorable than the standard error may potentially exhibit inhibitory activity against the RNAP from *M. tuberculosis*. In the protocol, RIF showed binding energy equal to -4.3 kcal/mol for the wild-type, which is in accordance with previous work where a binding energy of -4.96 kcal/mol was found for docking simulation (Kumar and Jena, 2014). On the other hand, a positive value of binding energy (56.6 kcal/mol) was found for the mutant form. Aiming to select only the compounds with the highest potential, only the hits showing binding energies more favorable than -10.0 kcal/mol were selected and analyzed. This binding energy value

Preprints (www.preprints.org) | NOT PEER-REVIEWED | Posted: 27 July 2017 doi:10.20944/preprints201707.0078.v1

was chosen as cut-off since it can be related to an inhibition constant in the namomolar range. In fact, the substitution of -10 kcal/mol in equation

$$Ki = \exp(\Delta G/RT)$$

(where Ki is the inhibition constant, ΔG is the binding energy, R is the gas constant and T is the temperature) results in an estimated inhibition constant of 89 nM. Tables 1 and 2 show the results of the screening for potential inhibitors of wtRNAP and mRNAP respectively. With the exception of remikiren (Clozel and Fischli, 1993), a renin inhibitor in development for the treatment of hypertension, the other compounds, anidulafungin (Denning, 2002), capreomycin (Johansen et al., 2006) and erythromycin (Jelić and Antolović, 2016), have antibiotic activity, although the targets involved in the pharmacological action are other than RNAP.

Table 1. Virtual screening results for the wild-type form of RNAP from *M. tuberculosis*. Only hits showing binding energies more favorable than –10.0 kcal/mol were selected (cutoff criteria).

DrugBank ID	Compound	Primary target	Binding energy (kcal/mol)
DB00362	Anidulafungin	glucan synthase[a]	-19.1
DB00314	Capreomycin	rRNA[b]	-14.3
DB00212	Remikiren	renin[c]	-11.3
DB01045	Rifampicin	RNA polymerase[d]	-4.3

[a](Denning, 2002)
[b](Johansen et al., 2006)
[c](Clozel and Fischli, 1993)
[d](Yarbrough et al., 1976)

Preprints (www.preprints.org) | NOT PEER-REVIEWED | Posted: 27 July 2017 doi:10.20944/preprints201707.0078.v1

Table 2. Virtual screening results for the mutant form of RNAP from *M. tuberculosis*. Only hits showing binding energies more favorable than –10.0 kcal/mol were selected (cutoff criteria).

DrugBank ID	Compound	Primary target	Binding energy (kcal/mol)
DB00199	Erythromycin	rRNA[a]	-17.5
DB00314	Capreomycin	rRNA[b]	-16.4
DB00212	Remikiren	renin[c]	-16.3
DB00362	Anidulafungin	glucan synthase[d]	-12.8
DB01045	Rifampicin	RNA polymerase[e]	56.6

[a](Jelić and Antolović, 2016)
[b](Johansen et al., 2006)
[c](Clozel and Fischli, 1993)
[d](Denning, 2002)
[e](Yarbrough et al., 1976)

4. CONCLUSIONS

In conclusion, seven strains of *M. tuberculosis* RIF resistant that present an insertion of four amino acids in RNA polymerase showed, a high biological cost. *In silico* study indicated that the insertion decreases the binding efficiency between RIF and mutant RNA when compared to the wild-type RNAP. With respect to wtRNAP, its interaction with RIF is analogous that observed in the crystallographic complex with the RNAP from *T. aquaticus*. Virtual screening showed four potential inhibitors for the mutant RNAP already approved for clinical use against other molecular targets: erythromycin, capreomycin, remikiren and anidulafungin.

CONFLICT OF INTEREST

The authors declare that there are no conflicts of interest.

 doi:10.20944/preprints201707.0078.v1

ACKNOWLEDGMENTS

Molecular graphics were performed with the UCSF Chimera package. Chimera is developed by the Resource for Biocomputing, Visualization, and Informatics at the University of California, San Francisco (supported by NIGMS P41-GM103311).

References

Almeida Da Silva, P.E.A., Palomino, J.C., 2011. Molecular basis and mechanisms of drug resistance in Mycobacterium tuberculosis: classical and new drugs. J. Antimicrob. Chemother. 66, 1417–30. doi:10.1093/jac/dkr173

Aloy, P., Ceulemans, H., Stark, A., Russell, R.B., 2003. The relationship between sequence and interaction divergence in proteins. J. Mol. Biol. 332, 989–98.

Altschul, S.F., Gish, W., Miller, W., Myers, E.W., Lipman, D.J., 1990. Basic local alignment search tool. J. Mol. Biol. 215, 403–410. doi:10.1016/S0022-2836(05)80360-2

Andersson, D.I., Hughes, D., 2010. Antibiotic resistance and its cost: is it possible to reverse resistance? Nat. Rev. Microbiol. 8, 260–71. doi:10.1038/nrmicro2319

Berendsen, H.J.C., Grigera, J.R., Straatsma, T.P., 1987. The missing term in effective pair potentials. J. Phys. Chem. 91, 6269–6271. doi:10.1021/j100308a038

Bergval, I., Kwok, B., Schuitema, A., Kremer, K., van Soolingen, D., Klatser, P., Anthony, R., 2012. Pre-Existing Isoniazid Resistance, but Not the Genotype of Mycobacterium Tuberculosis Drives Rifampicin Resistance Codon Preference in Vitro. PLoS One 7, e29108. doi:10.1371/journal.pone.0029108

Berman, H.M., 2000. The Protein Data Bank. Nucleic Acids Res. 28, 235–242. doi:10.1093/nar/28.1.235

BIADGLEGNE, F., RODLOFF, A.C., SACK, U., 2015. Review of the prevalence and drug resistance of tuberculosis in prisons: a hidden epidemic. Epidemiol. Infect. 143, 887–900. doi:10.1017/S095026881400288X

Borrell, S., Gagneux, S., 2009. Infectiousness, reproductive fitness and evolution of drug-resistant Mycobacterium tuberculosis. Int. J. Tuberc. Lung Dis. 13, 1456–66.

Brudey, K., Driscoll, J.R., Rigouts, L., Prodinger, W.M., Gori, A., Al-Hajoj, S.A., Allix, C., Aristimuño, L., Arora, J., Baumanis, V., Binder, L., Cafrune, P., Cataldi, A., Cheong, S., Diel, R., Ellermeier, C., Evans, J.T., Fauville-Dufaux, M., Ferdinand, S., Garcia de Viedma, D., Garzelli, C., Gazzola, L., Gomes, H.M., Guttierez, M.C., Hawkey, P.M., van Helden, P.D., Kadival, G. V, Kreiswirth, B.N., Kremer, K., Kubin, M., Kulkarni, S.P., Liens, B., Lillebaek, T., Ho, M.L., Martin, C., Martin, C., Mokrousov, I., Narvskaïa, O., Ngeow, Y.F., Naumann, L., Niemann, S., Parwati, I., Rahim, Z., Rasolofo-Razanamparany, V., Rasolonavalona, T., Rossetti, M.L., Rüsch-Gerdes, S., Sajduda, A., Samper, S., Shemyakin, I.G., Singh, U.B., Somoskovi, A., Skuce, R.A., van Soolingen, D., Streicher, E.M., Suffys, P.N., Tortoli, E., Tracevska, T., Vincent, V., Victor, T.C., Warren, R.M., Yap, S.F., Zaman, K., Portaels, F., Rastogi, N., Sola, C., 2006. Mycobacterium tuberculosis complex genetic diversity: mining the fourth international spoligotyping database (SpolDB4) for classification, population genetics and epidemiology. BMC Microbiol. 6, 23. doi:10.1186/1471-2180-6-23

Bussi, G., Donadio, D., Parrinello, M., 2007. Canonical sampling through velocity rescaling. J. Chem. Phys. 126, 14101. doi:10.1063/1.2408420

Campbell, E.A., Korzheva, N., Mustaev, A., Murakami, K., Nair, S., Goldfarb, A., Darst, S.A., 2001. Structural mechanism for rifampicin inhibition of bacterial rna polymerase. Cell 104, 901–12.

Campbell, E.A., Pavlova, O., Zenkin, N., Leon, F., Irschik, H., Jansen, R., Severinov, K., Darst, S.A., 2005. Structural, functional, and genetic analysis of sorangicin inhibition of bacterial RNA polymerase. EMBO J. 24, 674–682. doi:10.1038/sj.emboj.7600499

Chothia, C., Lesk, A.M., 1986. The relation between the divergence of sequence and

structure in proteins. EMBO J. 5, 823–6.

Clozel, J.P., Fischli, W., 1993. Discovery of remikiren as the first orally active renin inhibitor. Arzneimittelforschung. 43, 260–262.

Coelho, M.B., Costa, E.R.D., Vasconcellos, S.E.G., Linck, N., Ramos, R.M., Amorim, H.L.N. de, Suffys, P.N., Santos, A.R., Silva, P.E.A. da, Ramos, D.F., Silva, M.S.N., Rossetti, M.L.R., 2011. Sequence and structural characterization of tbnat gene in isoniazid-resistant Mycobacterium tuberculosis: identification of new mutations. Mutat. Res. 712, 33–9. doi:10.1016/j.mrfmmm.2011.03.017

Cole, S.T., 1996. Rifamycin resistance in mycobacteria. Res. Microbiol. 147, 48–52.

Colovos, C., Yeates, T.O., 1993. Verification of protein structures: patterns of nonbonded atomic interactions. Protein Sci. 2, 1511–9. doi:10.1002/pro.5560020916

Cui, Z., Wang, J., Lu, J., Huang, X., Zheng, R., Hu, Z., 2013. Evaluation of Methods for Testing the Susceptibility of Clinical Mycobacterium tuberculosis Isolates to Pyrazinamide. J. Clin. Microbiol. 51, 1374–1380. doi:10.1128/JCM.03197-12

Daley, C.L., Horsburgh, C.R., 2014. Editorial commentary: Treatment for multidrug-resistant tuberculosis: it's worse than we thought! Clin. Infect. Dis. 59, 1064–5. doi:10.1093/cid/ciu578

Dalla Costa, E.R., Ribeiro, M.O., Silva, M.S., Arnold, L.S., Rostirolla, D.C., Cafrune, P.I., Espinoza, R.C., Palaci, M., Telles, M.A., Ritacco, V., Suffys, P.N., Lopes, M.L., Campelo, C.L., Miranda, S.S., Kremer, K., da Silva, P., Fonseca, L., Ho, J.L., Kritski, A.L., Rossetti, M.L., 2009. Correlations of mutations in katG, oxyR-ahpC and inhA genes and in vitro susceptibility in Mycobacterium tuberculosis clinical strains segregated by spoligotype families from tuberculosis prevalent countries in South America. BMC Microbiol. 9, 39. doi:10.1186/1471-2180-9-39

Dalla Costa, E.R., Vasconcelos, S.E.G., Esteves, L.S., Gomes, H.M., Gomes, L.L., da Silva, P.A., Perdigão, J., Portugal, I., Viveiros, M., McNerney, R., Pain, A., Clark, T.G., Rastogi, N., Unis, G., Rossetti, M.L.R., Suffys, P.N., 2015. Multidrug-Resistant Mycobacterium tuberculosis of the Latin American Mediterranean Lineage, Wrongly Identified as Mycobacterium pinnipedii (Spoligotype International Type 863 [SIT863]), Causing Active Tuberculosis in South Brazil. J. Clin. Microbiol. 53, 3805–11. doi:10.1128/JCM.02012-15

Dallakyan, S., Olson, A.J., 2015. Small-Molecule Library Screening by Docking with PyRx. pp. 243–250. doi:10.1007/978-1-4939-2269-7_19

de Vos, M., Müller, B., Borrell, S., Black, P.A., van Helden, P.D., Warren, R.M., Gagneux, S., Victor, T.C., 2013. Putative compensatory mutations in the rpoC gene of rifampin-resistant Mycobacterium tuberculosis are associated with ongoing transmission. Antimicrob. Agents Chemother. 57, 827–32. doi:10.1128/AAC.01541-12

Denning, D.W., 2002. Echinocandins: a new class of antifungal. J. Antimicrob. Chemother. 49, 889–891. doi:10.1093/jac/dkf045

Diel, R., Nienhaus, A., Lampenius, N., Rüsch-Gerdes, S., Richter, E., 2014. Cost of multi drug resistance tuberculosis in Germany. Respir. Med. 108, 1677–1687. doi:10.1016/j.rmed.2014.09.021

Ebright, R.H., 2000. RNA Polymerase: Structural Similarities Between Bacterial RNA Polymerase and Eukaryotic RNA Polymerase II. J. Mol. Biol. 304, 687–698. doi:10.1006/jmbi.2000.4309

Essmann, U., Perera, L., Berkowitz, M.L., Darden, T., Lee, H., Pedersen, L.G., 1995. A smooth particle mesh Ewald method. J. Chem. Phys. 103, 8577–8593. doi:10.1063/1.470117

Eswar, N., Eramian, D., Webb, B., Shen, M.-Y., Sali, A., 2008. Protein structure modeling with MODELLER. Methods Mol. Biol. 426, 145–59. doi:10.1007/978-1-60327-058-8_8

Ferreira, L.G., Dos Santos, R.N., Oliva, G., Andricopulo, A.D., 2015. Molecular docking and structure-based drug design strategies. Molecules 20, 13384–421. doi:10.3390/molecules200713384

Frieden, T.R., Brudney, K.F., Harries, A.D., 2014. Global Tuberculosis. Jama 312, 1393. doi:10.1001/jama.2014.11450

Gandhi, N.R., Nunn, P., Dheda, K., Schaaf, H.S., Zignol, M., van Soolingen, D., Jensen, P., Bayona, J., 2010. Multidrug-resistant and extensively drug-resistant tuberculosis: a threat to global control of tuberculosis. Lancet 375, 1830–1843. doi:10.1016/S0140-6736(10)60410-2

Gasteiger, J., Marsili, M., 1980. Iterative partial equalization of orbital electronegativity?a rapid access to atomic charges. Tetrahedron 36, 3219–3228. doi:10.1016/0040-4020(80)80168-2

Ghosh, T., Bose, D., Zhang, X., 2010. Mechanisms for activating bacterial RNA polymerase. FEMS Microbiol. Rev. 34, 611–627. doi:10.1111/j.1574-6976.2010.00239.x

Gill, S.K., Garcia, G.A., 2011. Rifamycin inhibition of WT and Rif-resistant Mycobacterium tuberculosis and Escherichia coli RNA polymerases in vitro. Tuberculosis (Edinb). 91, 361–9. doi:10.1016/j.tube.2011.05.002

Guedes, I.A., de Magalhães, C.S., Dardenne, L.E., 2014. Receptor-ligand molecular docking. Biophys. Rev. 6, 75–87. doi:10.1007/s12551-013-0130-2

Herrera, L., Jiménez, S., Valverde, A., García-Aranda, M.A., Sáez-Nieto, J.A., 2003. Molecular analysis of rifampicin-resistant Mycobacterium tuberculosis isolated in

Spain (1996-2001). Description of new mutations in the rpoB gene and review of the literature. Int. J. Antimicrob. Agents 21, 403–8.

Hess, B., Bekker, H., Berendsen, H.J.C., Fraaije, J.G.E.M., 1997. LINCS: A linear constraint solver for molecular simulations. J. Comput. Chem. 18, 1463–1472. doi:10.1002/(SICI)1096-987X(199709)18:12<1463::AID-JCC4>3.0.CO;2-H

Hillisch, A., Pineda, L.F., Hilgenfeld, R., 2004. Utility of homology models in the drug discovery process. Drug Discov. Today 9, 659–69. doi:10.1016/S1359-6446(04)03196-4

Jelić, D., Antolović, R., 2016. From Erythromycin to Azithromycin and New Potential Ribosome-Binding Antimicrobials. Antibiotics 5, 29. doi:10.3390/antibiotics5030029

Johansen, S.K., Maus, C.E., Plikaytis, B.B., Douthwaite, S., 2006. Capreomycin Binds across the Ribosomal Subunit Interface Using tlyA-Encoded 2′-O-Methylations in 16S and 23S rRNAs. Mol. Cell 23, 173–182. doi:10.1016/j.molcel.2006.05.044

Kerrigan, J.E., 2013. Molecular dynamics simulations in drug design. Methods Mol. Biol. 993, 95–113. doi:10.1007/978-1-62703-342-8_7

Knox, C., Law, V., Jewison, T., Liu, P., Ly, S., Frolkis, A., Pon, A., Banco, K., Mak, C., Neveu, V., Djoumbou, Y., Eisner, R., Guo, A.C., Wishart, D.S., 2011. DrugBank 3.0: a comprehensive resource for “omics” research on drugs. Nucleic Acids Res. 39, D1035-41. doi:10.1093/nar/gkq1126

Kumar, S., Jena, L., 2014. Understanding Rifampicin Resistance in Tuberculosis through a Computational Approach. Genomics Inform. 12, 276. doi:10.5808/GI.2014.12.4.276

Laskowski, R.A., MacArthur, M.W., Moss, D.S., Thornton, J.M., 1993. PROCHECK: a program to check the stereochemical quality of protein structures. J. Appl.

Crystallogr. 26, 283–291. doi:10.1107/S0021889892009944

Law, V., Knox, C., Djoumbou, Y., Jewison, T., Guo, A.C., Liu, Y., Maciejewski, A., Arndt, D., Wilson, M., Neveu, V., Tang, A., Gabriel, G., Ly, C., Adamjee, S., Dame, Z.T., Han, B., Zhou, Y., Wishart, D.S., 2014. DrugBank 4.0: shedding new light on drug metabolism. Nucleic Acids Res. 42, D1091–D1097. doi:10.1093/nar/gkt1068

Liu, T., Tang, G.W., Capriotti, E., 2011. Comparative modeling: the state of the art and protein drug target structure prediction. Comb. Chem. High Throughput Screen. 14, 532–47.

Lüthy, R., Bowie, J.U., Eisenberg, D., 1992. Assessment of protein models with three-dimensional profiles. Nature 356, 83–5. doi:10.1038/356083a0

Malshetty, V., Kurthkoti, K., China, A., Mallick, B., Yamunadevi, S., Sang, P.B., Srinivasan, N., Nagaraja, V., Varshney, U., 2010. Novel insertion and deletion mutants of RpoB that render Mycobacterium smegmatis RNA polymerase resistant to rifampicin-mediated inhibition of transcription. Microbiology 156, 1565–1573. doi:10.1099/mic.0.036970-0

Minakhin, L., Bhagat, S., Brunning, A., Campbell, E.A., Darst, S.A., Ebright, R.H., Severinov, K., 2001. Bacterial RNA polymerase subunit and omega and eukaryotic RNA polymerase subunit RPB6 are sequence, structural, and functional homologs and promote RNA polymerase assembly. Proc. Natl. Acad. Sci. 98, 892–897. doi:10.1073/pnas.98.3.892

Molodtsov, V., Nawarathne, I.N., Scharf, N.T., Kirchhoff, P.D., Showalter, H.D.H., Garcia, G.A., Murakami, K.S., 2013. X-ray Crystal Structures of the Escherichia coli RNA Polymerase in Complex with Benzoxazinorifamycins. J. Med. Chem. 56, 4758–4763. doi:10.1021/jm4004889

Morris, G.M., Goodsell, D.S., Halliday, R.S., Huey, R., Hart, W.E., Belew, R.K., Olson, A.J., 1998. Automated docking using a Lamarckian genetic algorithm and an empirical binding free energy function. J. Comput. Chem. 19, 1639–1662. doi:10.1002/(SICI)1096-987X(19981115)19:14<1639::AID-JCC10>3.0.CO;2-B

Morris, G.M., Huey, R., Lindstrom, W., Sanner, M.F., Belew, R.K., Goodsell, D.S., Olson, A.J., 2009. AutoDock4 and AutoDockTools4: Automated docking with selective receptor flexibility. J. Comput. Chem. 30, 2785–2791. doi:10.1002/jcc.21256

Murakami, K.S., Darst, S.A., 2003. Bacterial RNA polymerases: the wholo story. Curr. Opin. Struct. Biol. 13, 31–9.

Murray, C.J.L., Ortblad, K.F., Guinovart, C., Lim, S.S., Wolock, T.M., Roberts, D.A., Dansereau, E.A., Graetz, N., Barber, R.M., Brown, J.C., Wang, H., Duber, H.C., Naghavi, M., Dicker, D., Dandona, L., Salomon, J.A., Heuton, K.R., Foreman, K., Phillips, D.E., Fleming, T.D., Flaxman, A.D., Phillips, B.K., Johnson, E.K., Coggeshall, M.S., Abd-Allah, F., Abera, S.F., Abraham, J.P., Abubakar, I., Abu-Raddad, L.J., Abu-Rmeileh, N.M., Achoki, T., Adeyemo, A.O., Adou, A.K., Adsuar, J.C., Agardh, E.E., Akena, D., Al Kahbouri, M.J., Alasfoor, D., Albittar, M.I., Alcalá-Cerra, G., Alegretti, M.A., Alemu, Z.A., Alfonso-Cristancho, R., Alhabib, S., Ali, R., Alla, F., Allen, P.J., Alsharif, U., Alvarez, E., Alvis-Guzman, N., Amankwaa, A.A., Amare, A.T., Amini, H., Ammar, W., Anderson, B.O., Antonio, C.A.T., Anwari, P., Arnlöv, J., Arsenijevic, V.S.A., Artaman, A., Asghar, R.J., Assadi, R., Atkins, L.S., Badawi, A., Balakrishnan, K., Banerjee, A., Basu, S., Beardsley, J., Bekele, T., Bell, M.L., Bernabe, E., Beyene, T.J., Bhala, N., Bhalla, A., Bhutta, Z.A., Abdulhak, A. Bin, Binagwaho, A., Blore, J.D., Basara, B.B., Bose, D., Brainin, M., Breitborde, N., Castañeda-Orjuela, C.A., Catalá-López, F.,

 doi:10.20944/preprints201707.0078.v1

Chadha, V.K., Chang, J.-C., Chiang, P.P.-C., Chuang, T.-W., Colomar, M., Cooper, L.T., Cooper, C., Courville, K.J., Cowie, B.C., Criqui, M.H., Dandona, R., Dayama, A., De Leo, D., Degenhardt, L., Del Pozo-Cruz, B., Deribe, K., Des Jarlais, D.C., Dessalegn, M., Dharmaratne, S.D., Dilmen, U., Ding, E.L., Driscoll, T.R., Durrani, A.M., Ellenbogen, R.G., Ermakov, S.P., Esteghamati, A., Faraon, E.J.A., Farzadfar, F., Fereshtehnejad, S.-M., Fijabi, D.O., Forouzanfar, M.H., Fra Paleo, U., Gaffikin, L., Gamkrelidze, A., Gankpé, F.G., Geleijnse, J.M., Gessner, B.D., Gibney, K.B., Ginawi, I.A.M., Glaser, E.L., Gona, P., Goto, A., Gouda, H.N., Gugnani, H.C., Gupta, R., Gupta, R., Hafezi-Nejad, N., Hamadeh, R.R., Hammami, M., Hankey, G.J., Harb, H.L., Haro, J.M., Havmoeller, R., Hay, S.I., Hedayati, M.T., Pi, I.B.H., Hoek, H.W., Hornberger, J.C., Hosgood, H.D., Hotez, P.J., Hoy, D.G., Huang, J.J., Iburg, K.M., Idrisov, B.T., Innos, K., Jacobsen, K.H., Jeemon, P., Jensen, P.N., Jha, V., Jiang, G., Jonas, J.B., Juel, K., Kan, H., Kankindi, I., Karam, N.E., Karch, A., Karema, C.K., Kaul, A., Kawakami, N., Kazi, D.S., Kemp, A.H., Kengne, A.P., Keren, A., Kereselidze, M., Khader, Y.S., Khalifa, S.E.A.H., Khan, E.A., Khang, Y.-H., Khonelidze, I., Kinfu, Y., Kinge, J.M., Knibbs, L., Kokubo, Y., Kosen, S., Defo, B.K., Kulkarni, V.S., Kulkarni, C., Kumar, K., Kumar, R.B., Kumar, G.A., Kwan, G.F., Lai, T., Balaji, A.L., Lam, H., Lan, Q., Lansingh, V.C., Larson, H.J., Larsson, A., Lee, J.-T., Leigh, J., Leinsalu, M., Leung, R., Li, Y., Li, Y., De Lima, G.M.F., Lin, H.-H., Lipshultz, S.E., Liu, S., Liu, Y., Lloyd, B.K., Lotufo, P.A., Machado, V.M.P., Maclachlan, J.H., Magis-Rodriguez, C., Majdan, M., Mapoma, C.C., Marcenes, W., Marzan, M.B., Masci, J.R., Mashal, M.T., Mason-Jones, A.J., Mayosi, B.M., Mazorodze, T.T., Mckay, A.C., Meaney, P.A., Mehndiratta, M.M., Mejia-Rodriguez, F., Melaku, Y.A., Memish, Z.A., Mendoza, W., Miller, T.R., Mills, E.J., Mohammad, K.A., Mokdad,

 doi:10.20944/preprints201707.0078.v1

A.H., Mola, G.L., Monasta, L., Montico, M., Moore, A.R., Mori, R., Moturi, W.N., Mukaigawara, M., Murthy, K.S., Naheed, A., Naidoo, K.S., Naldi, L., Nangia, V., Narayan, K.M.V., Nash, D., Nejjari, C., Nelson, R.G., Neupane, S.P., Newton, C.R., Ng, M., Nisar, M.I., Nolte, S., Norheim, O.F., Nowaseb, V., Nyakarahuka, L., Oh, I.-H., Ohkubo, T., Olusanya, B.O., Omer, S.B., Opio, J.N., Orisakwe, O.E., Pandian, J.D., Papachristou, C., Caicedo, A.J.P., Patten, S.B., Paul, V.K., Pavlin, B.I., Pearce, N., Pereira, D.M., Pervaiz, A., Pesudovs, K., Petzold, M., Pourmalek, F., Qato, D., Quezada, A.D., Quistberg, D.A., Rafay, A., Rahimi, K., Rahimi-Movaghar, V., Ur Rahman, S., Raju, M., Rana, S.M., Razavi, H., Reilly, R.Q., Remuzzi, G., Richardus, J.H., Ronfani, L., Roy, N., Sabin, N., Saeedi, M.Y., Sahraian, M.A., Samonte, G.M.J., Sawhney, M., Schneider, I.J.C., Schwebel, D.C., Seedat, S., Sepanlou, S.G., Servan-Mori, E.E., Sheikhbahaei, S., Shibuya, K., Shin, H.H., Shiue, I., Shivakoti, R., Sigfusdottir, I.D., Silberberg, D.H., Silva, A.P., Simard, E.P., Singh, J.A., Skirbekk, V., Sliwa, K., Soneji, S., Soshnikov, S.S., Sreeramareddy, C.T., Stathopoulou, V.K., Stroumpoulis, K., Swaminathan, S., Sykes, B.L., Tabb, K.M., Talongwa, R.T., Tenkorang, E.Y., Terkawi, A.S., Thomson, A.J., Thorne-Lyman, A.L., Towbin, J.A., Traebert, J., Tran, B.X., Dimbuene, Z.T., Tsilimbaris, M., Uchendu, U.S., Ukwaja, K.N., Uzun, S.B., Vallely, A.J., Vasankari, T.J., Venketasubramanian, N., Violante, F.S., Vlassov, V.V., Vollset, S.E., Waller, S., Wallin, M.T., Wang, L., Wang, X., Wang, Y., Weichenthal, S., Weiderpass, E., Weintraub, R.G., Westerman, R., White, R.A., Wilkinson, J.D., Williams, T.N., Woldeyohannes, S.M., Wong, J.Q., Xu, G., Yang, Y.C., Yano, Y., Yentur, G.K., Yip, P., Yonemoto, N., Yoon, S.-J., Younis, M., Yu, C., Jin, K.Y., El Sayed Zaki, M., Zhao, Y., Zheng, Y., Zhou, M., Zhu, J., Zou, X.N., Lopez, A.D., Vos, T., 2014. Global, regional, and national incidence and

mortality for HIV, tuberculosis, and malaria during 1990-2013: a systematic analysis for the Global Burden of Disease Study 2013. Lancet (London, England) 384, 1005–70. doi:10.1016/S0140-6736(14)60844-8

Oostenbrink, C., Villa, A., Mark, A.E., Van Gunsteren, W.F., 2004. A biomolecular force field based on the free enthalpy of hydration and solvation: The GROMOS force-field parameter sets 53A5 and 53A6. J. Comput. Chem. 25, 1656–1676. doi:10.1002/jcc.20090

Palomino, J.-C., Martin, A., Camacho, M., Guerra, H., Swings, J., Portaels, F., 2002. Resazurin microtiter assay plate: simple and inexpensive method for detection of drug resistance in Mycobacterium tuberculosis. Antimicrob. Agents Chemother. 46, 2720–2.

Parrinello, M., Rahman, A., 1981. Polymorphic transitions in single crystals: A new molecular dynamics method. J. Appl. Phys. 52, 7182–7190. doi:10.1063/1.328693

Pettersen, E.F., Goddard, T.D., Huang, C.C., Couch, G.S., Greenblatt, D.M., Meng, E.C., Ferrin, T.E., 2004. UCSF Chimera - A visualization system for exploratory research and analysis. J. Comput. Chem. 25, 1605–1612. doi:10.1002/jcc.20084

Pronk, S., Páll, S., Schulz, R., Larsson, P., Bjelkmar, P., Apostolov, R., Shirts, M.R., Smith, J.C., Kasson, P.M., Van Der Spoel, D., Hess, B., Lindahl, E., 2013. GROMACS 4.5: A high-throughput and highly parallel open source molecular simulation toolkit. Bioinformatics 29, 845–854. doi:10.1093/bioinformatics/btt055

Ramos, R.M., Perez, J.M., Baptista, L.A., De Amorim, H.L.N., 2012. Interaction of wild type, G68R and L125M isoforms of the arylamine-N-Acetyltransferase from mycobacterium tuberculosis with isoniazid: A computational study on a new possible mechanism of resistance. J. Mol. Model. 18. doi:10.1007/s00894-012-1383-6

Rapaport, D., 2013. The Art of Molecular Dynamics Simulation, 2nd Editio. ed. Cambridge University Press.

Rose, P.W., Prlic, A., Altunkaya, A., Bi, C., Bradley, A.R., Christie, C.H., Di Costanzo, L., Duarte, J.M., Dutta, S., Feng, Z., Green, R.K., Goodsell, D.S., Hudson, B., Kalro, T., Lowe, R., Peisach, E., Randle, C., Rose, A.S., Shao, C., Tao, Y.P., Valasatava, Y., Voigt, M., Westbrook, J.D., Woo, J., Yang, H., Young, J.Y., Zardecki, C., Berman, H.M., Burley, S.K., 2017. The RCSB protein data bank: Integrative view of protein, gene and 3D structural information. Nucleic Acids Res. 45, D271–D281. doi:10.1093/nar/gkw1000

Sanner, M.F., 1999. Python: a programming language for software integration and development. J. Mol. Graph. Model. 17, 57–61.

SAVES - The Structure Analysis and Verification Server [WWW Document], n.d. URL http://services.mbi.ucla.edu/SAVES/

Shen, M., Sali, A., 2006. Statistical potential for assessment and prediction of protein structures. Protein Sci. 15, 2507–2524. doi:10.1110/ps.062416606

Solis, F.J., Wets, R.J.-B., 1981. Minimization by Random Search Techniques. Math. Oper. Res. 6, 19–30. doi:10.1287/moor.6.1.19

Sotgiu, G., Centis, R., D'Ambrosio, L., Battista Migliori, G., 2015. Tuberculosis treatment and drug regimens. Cold Spring Harb. Perspect. Med. 5, a017822–a017822. doi:10.1101/cshperspect.a017822

Spies, F.S., von Groll, A., Ribeiro, A.W., Ramos, D.F., Ribeiro, M.O., Dalla Costa, E.R., Martin, A., Palomino, J.C., Rossetti, M.L., Zaha, A., da Silva, P.E.A., 2013. Biological cost in Mycobacterium tuberculosis with mutations in the rpsL, rrs, rpoB, and katG genes. Tuberculosis (Edinb). 93, 150–4. doi:10.1016/j.tube.2012.11.004

Strehl, E., 2014. [Multiple and extensive antibiotic resistance in Europe]. Med. Monatsschr. Pharm. 37, 347–8.

Supply, P., Allix, C., Lesjean, S., Cardoso-Oelemann, M., Rüsch-Gerdes, S., Willery, E., Savine, E., de Haas, P., van Deutekom, H., Roring, S., Bifani, P., Kurepina, N., Kreiswirth, B., Sola, C., Rastogi, N., Vatin, V., Gutierrez, M.C., Fauville, M., Niemann, S., Skuce, R., Kremer, K., Locht, C., van Soolingen, D., 2006. Proposal for standardization of optimized mycobacterial interspersed repetitive unit-variable-number tandem repeat typing of Mycobacterium tuberculosis. J. Clin. Microbiol. 44, 4498–510. doi:10.1128/JCM.01392-06

Telenti, A., Imboden, P., Marchesi, F., Lowrie, D., Cole, S., Colston, M.J., Matter, L., Schopfer, K., Bodmer, T., 1993. Detection of rifampicin-resistance mutations in Mycobacterium tuberculosis. Lancet (London, England) 341, 647–50.

Trott, O., Olson, A.J., 2009. AutoDock Vina: Improving the speed and accuracy of docking with a new scoring function, efficient optimization, and multithreading. J. Comput. Chem. 31, 455–461. doi:10.1002/jcc.21334

van Gunsteren, W.F., Dolenc, J., Mark, A.E., 2008. Molecular simulation as an aid to experimentalists. Curr. Opin. Struct. Biol. 18, 149–153. doi:10.1016/j.sbi.2007.12.007

van Soolingen, D., de Haas, P.E., Hermans, P.W., van Embden, J.D., 1994. DNA fingerprinting of Mycobacterium tuberculosis. Methods Enzymol. 235, 196–205.

Vassylyev, D.G., Sekine, S., Laptenko, O., Lee, J., Vassylyeva, M.N., Borukhov, S., Yokoyama, S., 2002. Crystal structure of a bacterial RNA polymerase holoenzyme at 2.6 Å resolution. Nature 417, 712–719. doi:10.1038/nature752

von Groll, A., Martin, A., Felix, C., Prata, P.F.S., Honscha, G., Portaels, F., Vandame, P., da Silva, P.E.A., Palomino, J.C., 2010a. Fitness study of the RDRio lineage and

Latin American-Mediterranean family of Mycobacterium tuberculosis in the city of Rio Grande, Brazil. FEMS Immunol. Med. Microbiol. 58, 119–27. doi:10.1111/j.1574-695X.2009.00611.x

von Groll, A., Martin, A., Portaels, F., Silva, P.E.A. da, Palomino, J.C., 2010b. Growth kinetics of Mycobacterium tuberculosis measured by quantitative resazurin reduction assay: a tool for fitness studies. Brazilian J. Microbiol. 41, 300–303. doi:10.1590/S1517-83822010000200006

WHO, 2016. WHO Global Tuberculosis Report 2016.

World Health Organization, 2010. Multidrug and extensively drug-resistant TB (M/XDR-TB) : 2010 global report on surveillance and response. World Health Organization, Geneva, 2010.

Zhang, Y., Yew, W.W., 2009. Mechanisms of drug resistance in Mycobacterium tuberculosis. Int. J. Tuberc. Lung Dis. 13, 1320–30. doi:10.2741/1289